Journal of Molecular Liquids 224 (2016) 792–800

Contents lists available at ScienceDirect

Journal of Molecular Liquids

journal homepage: www.elsevier.com/locate/molliq

Aqueous N-methylacetamide: New analytic potentials and a molecular dynamics study

Noelia Faginas-Lago[a,*], Andrea Lombardi[a], Margarita Albertí[b]

[a] Dipartimento di Chimica, Biologia e Biotecnologie, Università di Perugia, Via Elce di Sotto 8, Perugia 06123, Italy
[b] IQTCUB, Department de Ciencia de Materials i Química Física, Universitat de Barcelona, Barcelona, Spain

ARTICLE INFO

Article history:
Received 24 June 2016
Received in revised form 6 October 2016
Accepted 16 October 2016
Available online 19 October 2016

Keywords:
Intermolecular interactions
Molecular dynamics
H-bond interactions

ABSTRACT

Recently formulated intermolecular potentials for the N-methylacetamide-water system have been used to model the hydrogen-bond like interactions in classical molecular dynamics (MD) simulations of aqueous solutions of N-methylacetamide (NMA). The MD calculations have been performed covering a wide concentration range at a temperature of 308K, in order to validate the model potential through the reproduction of structural and dynamical properties of liquid NMA. The analytic intermolecular potential energy surface (PES), obtained by decomposing the involved molecules into a number of interacting centers, is represented as sum of van der Waals and electrostatic pair interaction terms. The van der Waals terms contain parameters directly connected to physical observables, such as atomic and bond polarizabilities, and can be easily optimized in order to embody more collective contributions such as hydrogen bonding like interactions. The parametrization is flexible enough to correctly match the electrostatic contributions, reproducing the results on N-methylacetamide solutions, as available from previous studies based on dynamics simulations and ab initio calculations. The use of the PES, combined with classical trajectories, provides a computationally effective alternative to ab initio MD simulations, widely used to simulate similar systems. Moreover, the characterization of the interacting centers is portable to different molecular environments, so that the PES can be extended for perspective applications to larger molecular systems and biomolecules.

1. Introduction

Modeling the hydrogen-bond (H-bond)-like interactions and understanding their role in the biomolecules is a fundamental issue in biochemistry and molecular biology. H-bonds occurring between different parts of the backbone of biomolecules (e.g. proteins) and between these and water molecules, contribute to the delicate balance of weak interactions stabilizing their complex structures, so driving molecular assembly and recognition processes, which are at the basis of the cell functioning [1]. Moreover, this topic deservedly attracts additional interest in connection to the question whether these interactions can be controlled and used in biotechnology applications to improve rational drug design [2] or in solid-state structure design [3], where the H-bonds can influence the packaging of solids to obtain desired chemical and physical properties.

In proteins, the interactions between different neighboring segments of the polypeptide backbone are established mainly by N–H···O=C hydrogen bonds. However, the C–H···O=C, C–H···π and C–H···N interactions, in spite of being weaker than standard hydrogen bonds, can play a determinant role in stabilizing intermolecular complexes, molecular structures and solutions [4–6], so that their knowledge might reveal to be crucial to gain insight into structure and properties of the biomolecules (see e.g. Refs. [2,7,8]).

Amides are simple molecular systems and useful prototypes to model both the strong H-bond interactions and the weaker ones (involving C–H bonds), since they can establish the different types of H-bond with water molecules in solutions and, at the same time, N–H···O=C H-bonds and C–H···O=C contacts in dimers [9–12]. Among amides, the N-methylacetamide, $CH_3CONHCH_3$ (NMA), is the simplest molecule that can be used as a model of the H-bond like interactions established between peptides and water and between different peptide centers.

Pure NMA is a colorless solid which melts just above room temperature (about 301 K) and boils at about 478 K. The temperature of melting, easily accessible, has allowed for numerous investigations of both its liquid phase and its water solutions (NMA is fairly soluble in water and organic solvents) [5,13–21]. The crystal structure of NMA, in turn, has been also widely investigated [22,23].

The theoretical studies of the effects of the H-bond interactions in liquid NMA and NMA-water solutions can be based on molecular dynamics (MD) simulations and serve as a model for the H-bond interactions in the biomolecules. Their validity depends on the

* Corresponding author.
E-mail address: noelia.faginaslago@unipg.it (N. Faginas-Lago).

http://dx.doi.org/10.1016/j.molliq.2016.10.077
0167-7322/

degree of accuracy of the description of the intermolecular interactions involving the N–H, O=C and C–H groups. In this respect, it must be mentioned that the very birth of H-bond interactions can be observed in gas phase, probing the interactions from a dynamical viewpoint through sensitive molecular beam scattering experiments involving water and other simple molecules containing hydrogen atoms [24] and subsequent validation through predictive dynamics calculations based on quantum and semiclassical methods (see e.g. [25,26]). Such experiments, assisted by theoretical methods for the interpretation of data, permitted to probe the H-bond formation and to obtain a wealth of results useful for an accurate modeling of the H-bond component of the intermolecular interactions [27,28].

Recently, NMA-NMA and NMA-water intermolecular potential energy surfaces (PESs), built following an approach based on the use of information obtained by molecular beam experiments and the related theoretical tools, have been developed and used in a study of the NMA dimer and the NMA-H_2O adduct [29]. A functional form introduced by Pirani et al. [24,30], tailored to accurately describe the non-electrostatic (van der Waals) interaction components [28,31] has been adopted to set up an analytic representation of the PES. This use of the Pirani function to represent the intermolecular interactions is well justified since it has been satisfactorily tested on various systems (see for instance Refs. [28,32-46]) and has proved to be suitable for modeling solvation and competitive interactions involving H_2O [47–50]. Here the same PESs of Ref. [29], originally developed for dimers, have been applied for the first time to a liquid system containing relatively complex molecules.

In the abovementioned previous work [29], we pointed out the tendency of the oxygen atoms of the NMA carbonyl groups to establish H-bonds with one of the H atom of the CH_3 methyl group, in the isolated NMA dimer (C=O$\cdots$H(CH_2) contacts). Also, a second stable geometry was found in which the oxygen of the NMA carbonyl group establishes a H-bond with the NH group (typical amide N–H$\cdots$O=C contacts). This marked a difference with the so far available results, obtained by using CHARMM22 and OPLS-AA charge distributions for NMA, since there only C=O$\cdots$H(CH_2) contacts were observed. On the other hand, it is known that crystallized NMA consists of chains of molecules in which hydrogen bonds between C=O and N–H groups connect adjacent molecules forming chains of hydrogen bond subunits [51]. Indeed, the role played by C=O$\cdots$H(CH_2) contacts in NMA has been previously considered (see Ref. [7]) observing that these interactions reinforces the N–H. . . O=C traditional interaction between NMA molecules, implying some stabilization of the chain packing [52].

In the present work MD simulations of neat NMA and NMA-water solutions at various concentrations are performed as a test ground for the appropriateness of the NMA-NMA and NMA-water intermolecular PESs. In the PES, the non-bonded interactions are expressed as a sum of NMA-NMA, NMA-H_2O and H_2O-H_2O interaction contributions [29] with the aim of assessing the reliability of our potentials for the study of H-bond interactions in aqueous environments and the perspective of extending our approach for applications to biomolecules. The abundance of data in the literature makes NMA a proper model system. Guided by the results obtained in our previous work [29], in the present study the AMBER charge distribution for NMA has been used [53].

The paper is structured as follows: in Section 2 we outline the formulation of the potential energy surface and in Section 3 details about the MD simulations are given. Results are presented and discussed in Section 4. Concluding remarks are given in Section 5.

2. The potential energy surface

The total potential energy of the NMA-water system for a given configuration, say V_{cfg}, is represented as a sum of an intramolecular part, V_{intra} (the PES of the isolated molecules) and an intermolecular energy contribution V_{inter}. Both contributions are calculated assuming the separability of electrostatic (including only permanent electric multipole contributions) and non-electrostatic interactions, whose corresponding potential energy terms are here denoted as V_{el} and V_{nel}, respectively. V_{nel} is the interaction component in general more difficult to formulate, since it results from the balance of dispersion and induction attraction forces, dominant at long range, and exchange (size) repulsion forces, dominant at short range.

For the non-electrostatic contribution to V_{intra} of the NMA molecule, we have followed the guidelines developed in a previous work [29], adopting the AMBER parameterization [53], including bond, angle and dihedral contributions. The non-electrostatic contribution to V_{intra} for the H_2O molecule is made up by harmonic otential energy functions for the bonds and the bending angle [28,54].

Regarding the intermolecular term V_{inter}, the non-electrostatic contributions come from NMA-NMA, H_2O-H_2O and NMA-H_2O pair interactions. Each of them has been represented as a sum of interaction contributions due to pairs of interacting centers (see Refs. [28,55]). In this picture, the molecules are made up by a number of interaction centers (depending on the complexity of the system), which can be placed on atoms, bonds or groups of atoms (for details about the choice of interacting centers see Refs. [55–57]). Five interaction centers have been placed on the NMA molecule, two of them on the C atoms of the two methyl groups, denoted as C_C and C_N to indicate the proximity of methyl groups to CO and NH bonds respectively (see Fig. 1), two on the C and O atoms of the carbonyl group and one, accounting for the NH group, on the N atom [28]. The interacting model for the H_2O molecule, instead, turned out to be much simpler because a single interaction center, placed on the O atom (denoted as Ow) and reproducing the overall effect of the two OH bonds and the two lone pairs, was adopted [58,59]. This assumption has been tested and validated in previous studies in which simulations of alkali ion aqueous solutions [36] were considered.

The total non-electrostatic potential, V_{nel}, is constructed as a sum over groups of ten, five and one interaction terms, accounting for NMA-NMA, NMA-H_2O and H_2O-H_2O intermolecular interactions respectively. Each effective pair contribution is defined by means of a Pirani potential function $V_P(r)$ [24,31,60], as follows:

$$V_P(r) = \varepsilon\left[\frac{m}{n(r)-m}\left(\frac{r_0}{r}\right)^{n(r)} - \frac{n(r)}{n(r)-m}\left(\frac{r_0}{r}\right)^{m}\right] \quad (1)$$

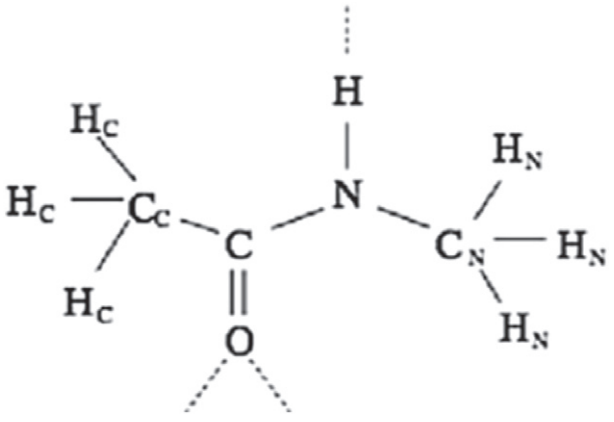

Fig. 1. The structure of NMA sketched as a peptide bond capped on both ends by a methyl group. Atoms belonging to the methyl group bonded to the carbonyl carbon are labeled by the subscript C (C_C), while those bonded to the nitrogen atom are labeled by the subscript N (C_N). The three hydrogen-bonding sites are marked with dashed lines.

In Eq. (1) ε, r_0 and m are pair specific parameters and r is the distance between the positions of the two interacting centers considered in the pair interaction. The first term of the bracketed sum in Eq. (1) (the positive one) represents the size-repulsion contribution arising from each pair, while the second term (negative) represents the effective dispersion attraction contribution for the given pair of centers. The exponent $n(r)$ of the first term modulates the falloff of the repulsion and controls the strength of the attraction as a function of r as follows:

$$n(r) = \beta + 4.0\left(\frac{r}{r_0}\right)^2 \tag{2}$$

with β being an adjustable parameter representing the hardness of the pair of interacting partners [31,60]. The introduction of this modulating parameter (not present in the standard Lennard-Jones function (LJ)) gives the possibility of indirectly taking into account some effects of the induction, charge transfer and atom clustering. The parameter β also corrects the dependence of the interaction on the internuclear distance, improving the LJ function in the asymptotic region [60]. For a full account of the advantages of the Pirani function see Refs. [31,36,60] and references therein. In the interactions between neutral molecules m is set equal to 6. A list of the parameters of the potential that have been used in the present work is given in Table 1. Quoted values have been derived from the polarizabilities of individual atoms or from effective group polarizabilities [29].

Once the separability of non-electrostatic and electrostatic contributions has been assumed, V_{nel} can be combined with any proper formulation of the electrostatic term V_{el}. In fact, the differences in the total configuration energy V_{cfg} due to the use of different formulations of V_{el}, can be compensated by properly modifying the parameter β. For instance, an increase of the permanent multipole moments, enhancing the attraction, can be compensated using higher values of β, thus increasing the repulsive character of the potential function, or in other words, the hardness. In the present study V_{el} is calculated as a sum of Coulombic interaction terms associated with a set of punctual charges localized on the interacting molecules following an appropriately defined spatial distribution. The charge distributions used in the present study for the NMA and water molecules have been adopted and validated in previous works [28,29,58,59]. In particular, twelve punctual charges, corresponding to the AMBER charge distribution, have been used for the NMA molecule [53], while three punctual charges whose distribution reproduces the appropriate dipole moment, μ, have been used for H_2O. The dipole moment μ has been taken equal to 2.43 D, which was proved to be adequate to simulate pure liquid water, with flexible molecules, setting the parameter β equal to 7.6 [28] (see Eq. (2)). This value of μ is consistent with charges of −0.87620 and 0.43810 a.u. placed on the O atom and the two H atoms, respectively.

Table 1
The values of the well depth (ε), equilibrium distance (r_0) and β parameters for the NMA-NMA, NMA-H_2O and H_2O-H_2O interactions.

Pairs	ε/meV	r_0/Å	β
NMA-NMA			
C_C–C_C	12.64	3.952	8.0
C_C–C_N	12.64	3.952	8.0
C_N–C_N	12.64	3.952	8.0
C–C	6.52	3.628	8.0
O–O	5.16	3.398	8.0
N–N	9.12	3.773	8.0
C_C–C	8.81	3.805	8.0
C_N–C	8.81	3.805	8.0
C_C–O	7.28	3.721	8.0
C_N–O	7.28	3.721	8.0
C_C–N	10.64	3.867	8.0
C_N–N	10.64	3.867	8.0
C–O	5.64	3.521	8.0
C–N	7.66	3.704	8.0
O–N	7.51	3.670	8.8
NMA-H_2O			
C_C–Ow	10.56	3.850	8.9
C_N–Ow	10.56	3.850	8.9
C–Ow	7.66	3.683	8.9
O–Ow	6.58	3.584	8.9
N–Ow	9.10	3.754	8.9
H_2O-H_2O			
Ow–Ow	9.06	3.730	7.6

3. Molecular dynamics simulations

The molecular dynamics simulations were carried out using the DL_POLY [61] molecular modeling package, conveniently modified to embody our interaction potential. Calculations involved a total of 512 molecules (NMA and water) placed in a cubic box. Water solutions of NMA, with molar fractions of NMA, denoted here as x_{NMA}, ranging from 1.0 to 0.4, have been simulated replacing each time the appropriate number of NMA molecules by H_2O molecules in the box. The simulations have been performed at temperature T = 308 K and pressure P = 1 atm, so adopting an isothermal-isobaric ensemble (NPT) and allowing for small expansions and contractions of the simulation cell. Specifically, we used the Berendsen NPT ensemble with thermostat and barostat relaxation times of 0.1 and 0.5 ps, respectively. A cutoff radius of 9.2 Å, a value established in previous works (see e.g. Ref. [36]), has been considered and such a truncation limit has been applied for the evaluation of the interaction (see Section 2). In practice, for any given molecule considered at the center of a sphere of radius 9.2 Å, only those having their center in the sphere are considered in computing the potential energy and the forces. Ewald lattice sums were used to evaluate Coulomb interactions (see Ref. [62]). The integration time step was set equal to 0.5 fs and particle positions and velocities were saved every 0.5 ps for analysis. The system was equilibrated for 1 ns (the data collected during equilibration are not included in final statistics) to ensure the absence of systematic oscillations in the potential energy. After the equilibration time, the simulation were run for 2 ns.

4. Results

4.1. Neat NMA

As a first step, neat liquid NMA has been considered, in order to understand, by comparison, the effects of adding water molecules to the solution. Changes in the liquid structure in going from neat NMA to less concentrated solutions have been followed by analyzing radial distribution functions $g(r)$ (RDFs) and distributions of specific angles formed by bonds of different NMA molecules (see below). The RDFs permit one to obtain information about the structure of a solid or a liquid, with the additional advantage of being connected to the structure factors extracted from X-ray and neutron diffraction measurements, in such a way allowing in principle for a direct comparison with this kind of experiments. Essentially, the radial distribution function can be interpreted as a probability of finding two particles at a distance r, giving information on particle spatial correlation. It can be constructed by considering a central particle and counting how many particles have their centers in a spherical shell from a distance r to a distance $r + dr$ from the center. Spanning a range of r values generates a histogram of the number of particles as a function of the distance from the center, from which a function denoted as $n(r)$ can be obtained and interpreted as a running coordination number. The typical trend of the RDF for a simple liquid is a sharp increase culminating at a maximum corresponding to the first neighbor shell and followed by a minimum at a distance $r = r_1$,

which marks the separation between first and second shells. Integrating $n(r)$ from $r = 0$ to r_1 gives a coordination number, which can be thought of as the number of particles surrounding any given one and included within the first solvation shell of approximate radius r_1. Since in liquids the particles at large distances are uncorrelated, the normalized RDF $g(r)$ for a liquid tends to 1 for $r \rightarrow \infty$. Indirectly, specific atom-pair RDFs, obtained from simulations, can be also compared to infrared spectroscopy (IR) experimental data, since the accuracy of the structural data (e.g. specific atom pair distances) can be validated in terms of the ability to reproduce the experimental spectra by spectral simulations.

An analysis of the spatial correlation of centers (e.g. specific atoms or groups) of different NMA molecules in pure NMA or in NMA aqueous solutions, contains structure information, which are the objects of the present work. In this case, the information is obtained calculating radial distribution functions for specific atom pairs, to identify the occurrence of H-bonds type interactions and related structural motifs.

As suggested by the NMA structure, qualitatively sketched in Fig. 1, one expects the intermolecular H-bond interactions of type N–H···O=C, established between pairs of NMA molecules, to lead to the formation and stability of H-bonded dimers, whose presence does actually characterize the structure of the neat NMA. The average number of N–H···O=C contacts that can be attributed to a single NMA molecule has been estimated by calculating the $g(r_{OH})$ RDF of the pairs given by an amide hydrogen atom (acting as donor) and a carbonyl oxygen atom (acceptor). Additional insight has been obtained from the $g(r_{NO})$ and $g(r_{OO})$ RDFs, containing information about nitrogen-oxygen and the oxygen-oxygen spatial correlation for pairs of NMA molecules, respectively. The three functions, calculated at T = 308 K and P = 1 atm, are shown in Fig. 2. In the upper panel, the $g(r_{OH})$ function exhibits a well pronounced first peak at a distance r ~1.9 Å and a second very broad one centered at r ~6.5 Å.

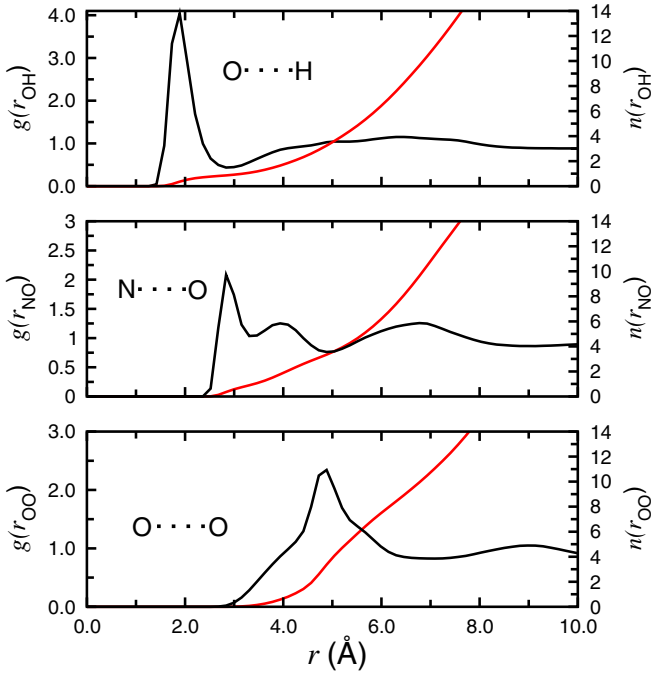

Fig. 2. $g(r_{OH})$ (upper panel), $g(r_{NO})$ (middle panel) and $g(r_{OO})$ (lower panel) radial distribution functions as obtained from simulations of neat NMA at P = 1 atm and T = 308 K. The coordination number as a function of the distance r is also shown (red line). The variable r_{OX} indicates O–X distances, where X stands for H (upper panel), N (middle panel) and O (lower panel) atoms respectively.

The first peak is sharp and is followed by a well defined minimum at r ~3.0 Å. The integration of the running coordination number function $n(r)$ (reported in the figure as a red line) over the peak (i.e. from $r = 0$ to $r = 3.0$, see above) yields a coordination number of about 1, which indicates the presence of one hydrogen bond contact, coordinating the NMA carbonyl oxygen and the amide hydrogen of neighbor molecules. This results are in substantial agreement to those obtained by Whitfield et al. in their theoretical work on the liquid NMA structure [52] (based on molecular dynamics simulations) and by Zhang et al. [5] (based on molecular dynamics simulations and NMR experiments) both reporting the values of 1.9 and 6.5 Å for the first and second peak positions, respectively. Agreement is also found with the distances and peak positions that can be gathered from the intermolecular pair-correlation functions of Ref. [63] obtained from the analysis of X-ray and neutron scattering measurement data.

In the middle panel of Fig. 2, the $g(r_{NO})$ function exhibits a first peak centered at r ~2.8 Å and a well distinguished minimum at r ~3.5 Å, in substantial agreement with the average N–O distance value, obtained from ab initio calculations, given in Ref. [64], where a validation by comparison with IR spectra was made and in Ref. [65], by the same author, where analogous improved theoretical results were compared to both IR and nuclear magnetic resonance experimental data. The integration of the running coordination number function $n(r)$ (red line) over this peak returns a coordination number equal to 1. This result indicates the amide hydrogen of the NMA acting as a donor in a single H-bond and is in good agreement with the conclusions drawn in Ref. [66], where dimers and trimers with a single H-bond are found to be best structural motifs to be assumed for reproducing by theory X-ray scattering data of liquid NMA at 308 K and where N–O distances ranging from 2.9 to 3.0 Å have been estimated. Agreement is found also with a more recent experimental study [63] based on neutron and X-ray diffraction measurements.

The comparison of the first peak positions of the $g(r_{OH})$ and $g(r_{NO})$ RDFs suggests that the N and H atoms, belonging to the amide group, and the carbonyl oxygen must be typically nearly linearly aligned in dimers formed by pairs of NMA molecules, forming an angle of about 180°. To further verify this conclusion, we calculated the distribution of the cosine of the $\hat{NHO}$ angle, here denoted as θ, formed by the N–H bond of the amide center and the line connecting the H atom and the carbonyl oxygen of neighbor pairs of molecules, where neighbor pairs are defined as those for which the distance between the amide hydrogen and the carbonyl oxygen is lower than 3 Å, as suggested by the position of the first minimum of the $g(r_{OH})$ RDF (upper panel of Fig. 2). The angle θ is explicitly calculated as the one formed by two vectors starting from the hydrogen atom position and pointing towards the nitrogen and oxygen atoms respectively. Fig. 3 shows the distribution of cosθ formed by hydrogen-bonded neighbor pairs, compared to the equivalent distribution for non-bonded pairs (for convenience the abscissa axis reports the values of the corresponding angle, instead of its cosine). It can be seen that NMA molecules of the hydrogen-bonded pairs tends to form angles ranging from 120 and 180°, not surprisingly given the somewhat directional character of the H-bond interactions. A just qualitative picture of the arrangement of the NMA molecules in a H-bonded dimer in solution is represented in Fig. 4.

The previous comparisons and the dimer arrangement help us to interpret the $g(r_{OO})$ RDF, which actually shows two main peaks, the first one being a shoulder in the RDF profile at r ~4.5 Å, while the main peak is at r ~=4.9 Å. This RDF is also similar to that found by Whitfield et al. [52], but less structured between the first and second peak and very similar to that reported in Ref. [11]. As it has been commented in Ref. [52], the shape of this function indicates the presence of a significant number of O–O contacts at distances significantly lower than 4.9 Å, indicating that in liquid phase shorter contacts are present (the shortest O–O distance within the hydrogen-bonded chains in solid NMA is of 4.9 Å [67]). Short O–O contacts observed

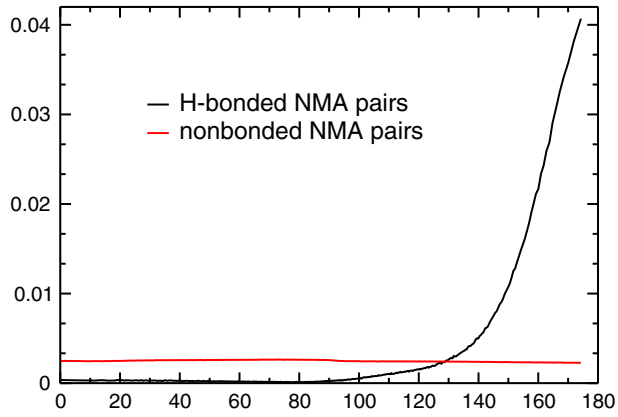

Fig. 3. Comparison of the distributions of the cosine of the NĤO angle θ formed by H-bonded and non-bonded neighbor NMA pairs, as obtained from simulations of neat NMA at P = 1 atm and T = 308 K (for convenience, the values of the angle are indicated, instead of its cosine).

for liquid NMA can certainly be attributed to some degree of disorder characterizing liquid NMA with respect to the crystal [52]. The shallow minimum between the first and second maxima indicates that there is a significant fraction of NMA molecules for which there is low correlation in the O–O positions and for which O–O contacts must arise from non-bonded molecules.

4.2. Water solutions of NMA

After a characterization of the liquid neat NMA, the intermolecular potential energy has been upgraded including the interaction terms accounting for the NMA-H_2O and H_2O-H_2O contributions in order to simulate solutions of NMA and water. The solutions have been simulated at P = 1 atm and T = 308 K (see Section 3), for different values of the NMA molar fractions, x_{NMA} = 0.4, 0.6 and 0.8. An analysis of the effects of the presence of water molecules on the structure of the solution has been carried out to validate the potential energy function. To this aim, the spatial correlation of carbonyl oxygen and amide hydrogen for pairs of NMA molecules and the spatial correlation of the NMA carbonyl oxygen with the hydrogen and oxygen atoms of water molecules have been characterized. The obtained results are illustrated in the following sections.

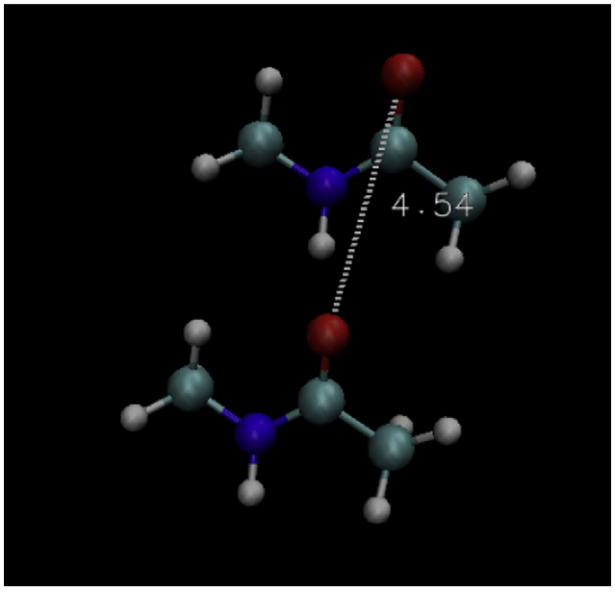

Fig. 4. Qualitative sketch of H-bonded dimer structure in neat liquid NMA, as suggested from the analysis of the RDF functions shown in Fig. 2 with O–O contact peak at distances r between ~4.5 and 5.5 Å.

4.2.1. Contacts between NMA molecules

The occurrence of H-bond interactions between NMA molecules in water solutions has been investigated calculating the $g(r_{OH})$, the $g(r_{NO})$ and the $g(r_{OO})$ RDFs and comparing them with the analogue ones obtained from neat NMA simulations.

The $g(r_{OH})$ functions for NMA-water solutions are shown in Fig. 5, for each of the values of the molar fraction x_{NMA}. The effect of the dilution is visible in the slight displacements of the first peak positions in the $g(r_{OH})$ functions towards shorter distances, as x_{NMA} decreases (namely for increasing water concentrations), which indicates a certain strengthening of the single contacts of type N–H···O=C, involving the carbonyl oxygen and the amide hydrogen. Accordingly, it has been also observed a decrease of the coordination number, from a value of ≃1.0 for the most concentrated solution investigated, x_{NMA} = 0.8 (a value of 1.0 is found for neat NMA, see previous Section 4.1), to a value of 0.43 for x_{NMA} = 0.4. The decrease of the number of O–H contacts with H-bond character is reflected in the progressively smaller coordination number obtained from the RDF functions of Fig. 5, for decreasing values of x_{NMA}. The second peak of the $g(r_{OH})$ is shifted as well towards lower values of the distance r, for decreasing NMA molar fractions. The contraction of the second shells, characterizing the trend of the $g(r_{OH})$ functions, reflects the effect of the smaller size of the water molecule with respect to that of NMA, allowing for a shorter average distance between NMA molecules. Since the probability of finding NMA molecules separated by shorter distances is higher for the most diluted solutions, the second peak is more structured for lower x_{NMA} values.

The function $g(r_{NO})$, also containing information on N–H···O=C H-bond contacts, is represented in the middle panel of Fig. 5. As in

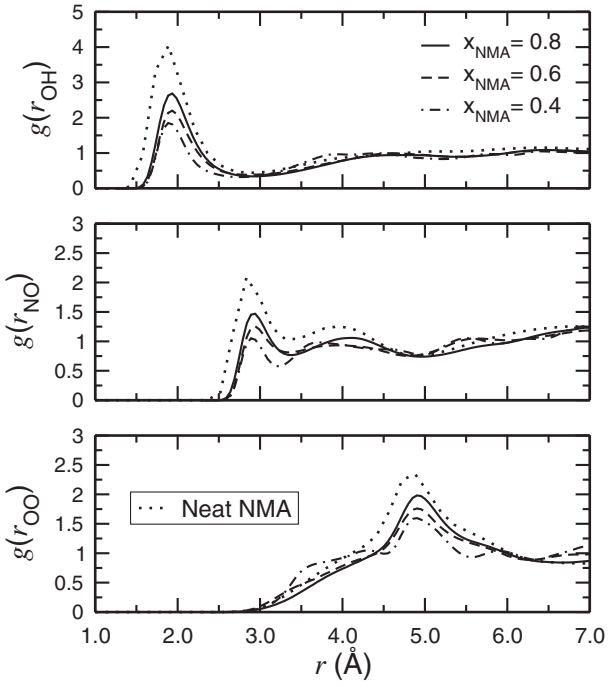

Fig. 5. $g(r_{OH})$ (upper panel), $g(r_{NO})$ (middle panel) and $g(r_{OO})$ (lower panel) radial distribution functions of NMA-water solutions, accounting for interactions between the amide hydrogen and carbonyl oxygen of pairs of NMA molecules at different NMA molar fractions, as indicated in the legend. The corresponding RDFs for neat NMA are also shown for comparison (dotted lines).

the case of OH contacts, the first peak of the $g(r_{NO})$ function is shifted towards shorter distances, with respect to the analogue RDF for neat NMA, for lower NMA concentrations and, at the same time, its intensity (and area) decreases. Moreover, as for $g(r_{OH})$, we observe a more structured second peak at lower concentrations. This effects can be attributed again to the smaller volume occupied by water molecules, with respect to the NMA ones, that promotes much closer contacts between NMA molecules.

Regarding the $g(r_{OO})$ RDFs, shown in the lower panel of Fig. 5, we observe that the functions are increasingly much rich of features, as x_{NMA} decreases, with respect to the ones shown in the lower panel of Fig. 2, where O–O contacts for neat NMA are shown. The functions have a main peak around r ~4.9 Å and are more structured at shorter distances for lower NMA concentrations. This can be explained considering that within this distance range, the presence of water molecules perturbs the original distribution of O–O contacts observed for neat NMA.

As for neat NMA (see Section 4.1), we calculated the distribution of the cosine of the NĤO angle θ, formed by the N–H bond of the amide center and the carbonyl oxygen of neighbor pairs of NMA molecules, where neighbor pairs are again defined as those for which the distance between the amide hydrogen and the carbonyl oxygen is less than 3 Å (following the same definition adopted for neat NMA, see Section 4.1). Fig. 6 shows the cosθ distributions as obtained from simulations at T = 308 K and P = 1 atm for x_{NMA} = 0.4, 0.6 and 0.8, and compares them with the corresponding distribution for nonbonded NMA pairs (for convenience the abscissa axis reports the values of the corresponding values of the θ angle, in place of its cosine). The shape of the distribution functions for H-bonded NMA pairs is similar to the one obtained for neat NMA and shown in Fig. 3, indicating that the presence of water molecules does not substantially alter the dimer geometry.

4.2.2. Contacts between NMA and H_2O molecules

The aqueous solutions of NMA are characterized by the possible formation of H-bonds between the amide hydrogen atom of the NMA and the oxygen atom of the H_2O molecules (here denoted as Ow). Moreover contacts involve the carbonyl oxygen atom of the NMA and the hydrogen atoms (denoted as Hw) of H_2O. The occurrence of these contacts has been investigated by analyzing the $g(r_{HOw})$ and $g(r_{HwO})$ RDFs. Further insight has been obtained from the analysis of the $g(r_{OOw})$ functions.

The H-bond formation with NMA acting as a hydrogen donor, when water is involved, is reflected in the $g(r_{HOw})$ functions, which have been obtained from simulations at P = 1 atm and T = 308 K for x_{NMA} = 0.4, 0.6 and 0.8 and are displayed in the lower panel of Fig. 7. The figure shows the first peak of each function centered at a distance r ~2.0 Å, which is characteristic of established hydrogen bond contacts. It can be seen that the H–Ow correlation decreases (lower height of the peaks) for decreasing values of x_{NMA}. A second broad peak, more structured at the lower NMA concentrations, is observed between r ~5.0 and r ~6.0 Å. This second peak is attributed to the interactions between the amide H atom of the NMA and the Ow atoms of water molecules participating in carbonyl oxygen-H_2O contacts. The structure of such peak is enriched by a shoulder at distances between ~3.0 and ~4.0 Å, which can be attributed to amide hydrogen-H_2O-H_2O contacts, suggesting that a variety of different NMA-H_2O structural motifs, with a signature in the $g(r_{HOw})$ profile, contributes to characterize NMA water solutions.

The H-bond formation with NMA acting as a hydrogen acceptor has been also investigated, considering the $g(r_{HwO})$ radial distribution functions shown in the middle panel of Fig. 7. As for the $g(r_{HOw})$ RDFs, this functions display the characteristic peaks of the hydrogen bonding at distances progressively shorter than ~1.9 Å for decreasing values of x_{NMA}. A smaller second peak at a distance r ~3.2 Å can be explained as due to the second hydrogen atom of the H-bonded water molecule. These values obtained for the $g(r_{HwO})$ first and second peak positions are in fair agreement with those obtained by Zhang et al. in Ref. [5] by MD calculations (~1.8 and ~3.3, respectively) and in Ref. [68] by density functional theory (DFT) calculations compared to IR experimental data (~1.9 Å for the average O–Hw contact distance). A third broad peak at distances between ~5.0 and

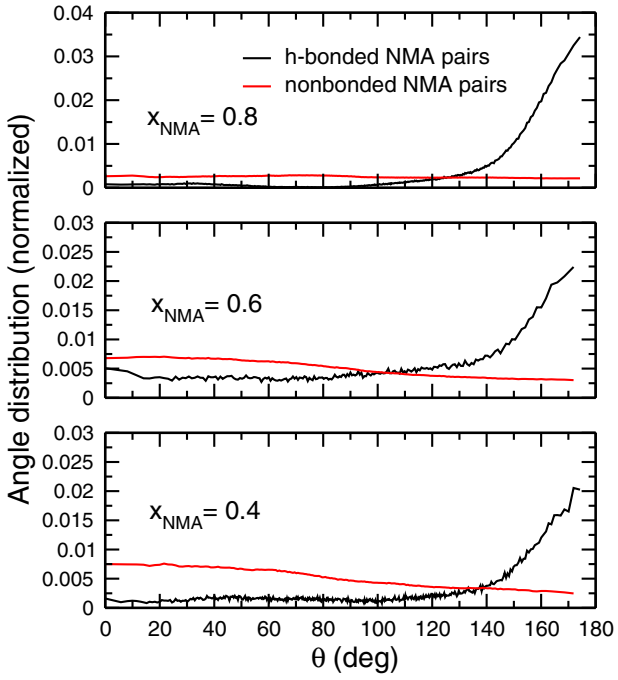

Fig. 6. Comparison of the distributions of the cosine of the NĤO angle θ formed by H-bonded and non-bonded neighbor NMA pairs, as obtained from simulations of NMA and water at P = 1 atm and T = 308 K and for x_{NMA} = 0.4, 0.6 and 0.8 (for convenience, the values of the angle are indicated, instead of its cosine).

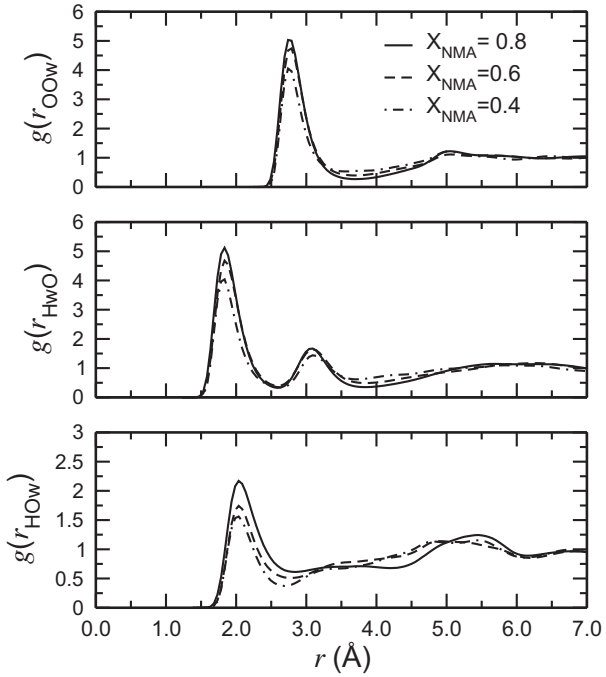

Fig. 7. $g(r_{OOw})$ (upper panel), $g(r_{HwO})$ (middle panel) and $g(r_{HOw})$ (lower panel) radial distribution functions, accounting for interactions between the amide hydrogen of the NMA molecule and water oxygen, as obtained from simulations at T = 308 K and P = 1 atm. The legend indicates the molar fraction of the NMA.

7.0 Å, indicates an abundance of O–Hw contacts and can be explained as due to the correlation between the carbonyl oxygen and water molecules accepting a hydrogen bond from the amide group, which are lying at the opposite side of the NMA backbone.

The $g(r_{OOw})$ RDFs, accounting for the O–Ow correlation, are displayed in the upper panel of Fig. 7. The figure shows that the first peaks of the RDFs are centered approximately at r ~2.8 Å in good agreement with the O–Ow contact average distance of ~2.85 *Å* reported in Ref. [68] and with the peak position of the analogous RDFs reported by Allison et al. [11]. A second peak is present in the RDFs at r ~5.0 Å. The first peak is clearly due to the presence of water molecules, which establish H-bond contacts with the carbonyl oxygen of NMA, i.e. to hydrogen bonded configurations where the NMA molecule acts as an acceptor of one or more water hydrogen. The second peak is due to O–Ow contacts involving water molecules with a contact with the amide hydrogen atom of the NMA molecules, acting as a hydrogen bond donor. The minimum between the two peaks becomes shallower when the NMA concentration decreases, suggesting again that a variety of different NMA-H_2O structural motifs can contribute to the peak at 5.0 *Å* of the $g(r_{OOw})$ RDF.

The donor and acceptor role of NMA is illustrated qualitatively in Fig. 8, where a snapshot from simulations shows a single NMA molecule with three hydrogen-bonded water neighbors. The dashed white lines and numbers and letters refer to distances corresponding to some of the types of water-NMA coordination considered above.

Additional analogous results on NMA-water solutions available in the literature, where $g(r_{HwO})$, $g(r_{HOw})$ and $g(r_{OOw})$ RDFs [12,69,70] (mostly treating more diluted solutions) are also in substantial qualitative agreement with the above exposed results.

5. Conclusions

A potential energy surface originally developed for NMA-NMA and NMA-water dimers, has been used here to model the intermolecular interactions occurring in the NMA-water system and to perform MD simulations. The study was targeted to the description of the H-bond interactions characterizing the liquid structure of neat NMA and NMA aqueous solutions, with the aim of validating the interaction model through comparison with previous available theoretical studies. The PES has been formulated as a sum of Coulombic electrostatic terms and van der Waals terms, the latter accounting for pairs of interaction centers properly placed on the NMA and water molecules. The parameters used in the potential terms have a clear physical meaning and have been optimized to embody more delocalized contributions and to render the pair components of more collective effects like those characterizing hydrogen bonding, particle clustering and bond or atom group dipole moments.

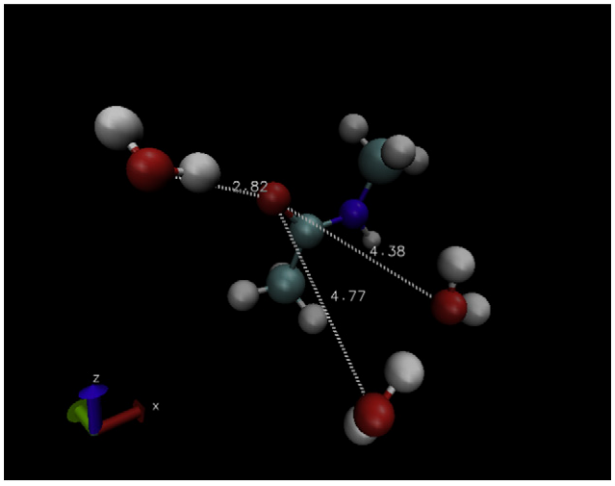

Fig. 8. A snapshot taken from a simulation of water and NMA at $x_{NMA} = 0.4$, P = 1 atm and T = 308 K, showing a single NMA molecule with three hydrogen-bonded water neighbors and a second nearest neighbor water connected to the NMA by two hydrogen bonds. The dashed white lines and numbers indicate distances between oxygen atoms.

Neat NMA and water solutions have been simulated at a temperature T = 308 K and a pressure P = 1 atm, analyzing the NMA-NMA contacts of H-bond type through the calculation of NH···C=O, N–O and O–O atom pair radial distribution functions and H-bond angle distributions. Similar calculations have been performed for NMA-H_2O H-bond type contacts. A wide range of concentrations (including neat NMA) has been covered. The picture of the O–H contacts extracted from the RDFs for NMA-NMA dimers indicates a tendency to form a single H-bond between neighbor NMA molecules at a characteristic distance of ~1.9 Å, in fair agreement with most of the previous theoretical studies. This interaction has a certain directional character, which is reflected in the $\hat{NHO}$ angle distribution, peaked between 140 and 180°. Only a slight contraction of the first shell is found in the NMA aqueous solutions, when NMA-NMA contacts are analyzed by the RDFs, indicating that the typical NH···O=C interaction is not affected by the presence of water molecules in the considered concentration range. The contacts of NMA with water molecules involve both the carbonyl oxygen and the amide hydrogen. The $g(r_{HOw})$ RDFs show that the typical distance for NH···Ow contacts is 2.0 Å and that for a fraction of NMA molecules the amide hydrogen interacts with two water oxygen atoms, although at distances larger than 3 Å. The presence of CO···Hw contacts, at a typical distance of ~1.9 Å has been also documented by $g(r_{HwO})$ and $g(r_{OOw})$ RDFs.

The various van der Waals pair interaction terms of the PES have been modeled by Pirani potential functions, explicitly connected to atomic and bond polarizabilities, namely physical quantities which add up to reproduce the overall molecular polarizability. For this reason the interaction terms are portable to larger molecules with similar interacting centers, to some extent regardless of the molecular dimensions. The PES can therefore be promptly extended to reproduce the interaction of larger molecules for perspective use in the theoretical study of biomolecules, on the basis of the overall consistency of the results here obtained.

Acknowledgments

N. F.-L. acknowledges financial support from Fondazione Cassa di Risparmio di Perugia (P 2014/1255, ACT 2014/6167) and the OU Supercomputing Center for Education & Research (OSCER) at the University of Oklahoma (OU) for the computing time. M. A. acknowledges financial support from the Ministerio de Educación y Ciencia (Spain, Project CTQ2013-41307-P) and the Generalitat de Catalunya (2009SGR-17). A. L. acknowledges financial support from the Dipartimento di Chimica, Biologia e Biotecnologie dell'Università di Perugia (FRB, Fondo per la Ricerca di Base), from MIUR PRIN 2010–2011 (contract 2010ERFKXL_002) and from "Fondazione Cassa Risparmio Perugia (Codice Progetto: 2015.0331.021 Ricerca Scientifica e Tecnologica)".

References

[1] T. Liu, H. Li, M. Huang, Y. Duan, Z. Wang, Two-way effects between hydrogen bond and intramolecular resonance effect: an ab initio study on complexes of formamide and its derivatives with water, J. Phys. Chem. A 112 (2008) 5436–5447.
[2] G.R. Desiraju, C-H···O and other weak hydrogen bonds. From crystal engineering to virtual screening, Chem. Commun. (2005) 2995–3001.
[3] G.R. Desiraju, J.J. Vittal, A. Ramanan, Crystal Engineering. A Textbook, World Scientific Publishing, Singapore, 2011.
[4] R. Vargas, J. Garza, R.A. Friesner, H. Stern, B.P. Hay, D.A. Dixon, Strength of the N-H centered dots O=C and C-H centered dots O=C bonds in formamide and N-methylacetamide dimers, J. Phys. Chem. A 105 (2001) 4963–4968.

[5] R. Zhang, H. Li, Y. Lei, S. Han, Different weak CH···O contacts in N-methylacetamide-water system: molecular dynamics simulations and NMR experimental study, J. Phys. Chem. B 108 (2004) 12596–12601.
[6] R. Zhang, H. Li, Y. Lei, S. Han, All-atom molecular dynamic simulations and relative NMR spectra study of weak CH···O contacts in amide-/water systems, J. Phys. Chem. B 109 (2005) 7482–7487.
[7] T. Whitfield, J. Crain, G. Martyna, Structural properties of liquid N-methylacetamide via ab initio, path integral and classical molecular dynamics, J. Chem. Phys. 124 (2006) 094503.
[8] S. Steiner, G.R. Desiraju, The Weak Hydrogen Bond, Oxford: University Press, USA, 1999,
[9] I.M. Klotz, J.S. Franzen, Hydrogen bonds between model peptide groups in solution, J. Am. Chem. Soc. 84 (1962) 3461–3466.
[10] T. Whitfield, G.J. Martyna, S. Allison, S.P. Bates, J. Crain, Liquid NMA: a surprisingly realistic model for hydrogen bonding motifs in proteins, Chem. Phys. Lett. 414 (2005) 210–214.
[11] S.K. Allison, A.P. Bates, J. Crain, G.J. Martyna, Solution structure of the aqueous model peptide N-methylacetamide, J. Phys. Chem. B 110 (2006) 21319–21326.
[12] Y.A. Mantz, H. Gerard, R. Iftimie, G.J. Martyna, Isomerization of a peptidic fragment studied theoretically in vacuum and in explicit water solvent at finite temperature, J. Am. Chem. Soc. 126 (2004) (4081–4081).
[13] M. Omar, Dielectric properties of pure liquid N-methylacetamide, J. Chem. Soc. Faraday Trans. I 76 (1980) 711–716.
[14] Fourier transform near-infrared spectra of N-methylacetamide: dissociation and thermodynamic properties in pure liquid form and in CCl4 solutions, Appl. Spectrosc. 48 (9) (1994) 1095–1101.
[15] D. Turton, K. Wynne, Structural relaxation in the hydrogen-bonding liquids N-methylacetamide and water studied by optical Kerr effect spectroscopy, J. Chem. Phys. 128 (15) (2008) 154516.
[16] H. Minami, M. Iwahashi, Molecular self-assembling of N-methylacetamide in solvents, Int. J. Spectr. 2011 (2011) (640121(1)–640121(7)).
[17] M. Czarnecki, K. Haufa, Effect of temperature and concentration on the structure of N-methylacetamide-water complexes: near-infrared spectroscopic study, J. Phys. Chem. A 109(6) (2005) 1015–1021.
[18] K. Kwac, M. Cho, Amide I modes in the N-methylacetamide dimer and glycine dipeptide analog: diagonal force constants, J. Chem. Phys. 119 (2003) 2256–2263.
[19] J. Caldwell, P. Kollman, Structure and properties of neat liquids using nonadditive molecular dynamics: water, methanol, and N-methylacetamide, J. Chem. Phys. 99 (1995) 6208–6219.
[20] V. Giordani, V. Bryantsev, J. Uddin, W. Walker, G.V. Chase, D. Adisson, ECS Electrochem. Lett. 3 (2014) 11–14.
[21] S. Pattanayak, S. Chowdhurl, Effects of methanol on the hydrogen bonding structure and dynamics in aqueous N-methylacetamide solution, J. Mol. Liq. 194 (2014) 141–148.
[22] M. Barthes, H. Bordallo, J. Eckert, O. Maurus, G. Nunzio, J. de Léon, Dynamics of crystalline N-methylacetamide: temperature dependence of infrared and inelastic neutron scattering spectra, J. Phys. Chem. B 102 (1998) 6177–6183.
[23] J. Eckert, M. Barthes, W. Klooster, A. Albinati, R. Aznar, T. Koetzle, No evidence for proton transfer along the N-H···O hydrogen bond in N-methylacetamide: neutron single crystal structure at 250 and 276 K, J. Phys. Chem. B 105 (2001) 19–24.
[24] A.F. Albernaz, V. Aquilanti, P.R.P. Barreto, C. Caglioti, A.C.P.S. Cruz, G. Grossi, A. Lombardi, F. Palazzetti, Interactions of hydrogen molecules with halogen-containing diatomics from ab initio calculations: spherical-harmonics representation and characterization of the intermolecular potentials, J. Phys. Chem. A 120 (2016) 5315–5324.
[25] N. Faginas-Lago, F. Huarte-Larrañaga, A. Laganà, Full dimensional quantum versus semiclassical reactivity for the bent transition state reaction $N + N_2$, Chem. Phys. Lett. 464 (4–6) (2008) 249–255.
[26] A. Laganà, N. Faginas-Lago, S. Rampino, F. Huarte-Larrañaga, E. García, Thermal rate coefficients in collinear versus bent transition state reactions: the $N_2 + N_2$ case study, Phys. Scr. 78 (5) (2008) 058116.
[27] V. Aquilanti, E. Cornicchi, M. Moix Teixidor, N. Saendig, F. Pirani, D. Cappelletti, Glory-scattering measurement of water-noble-gas interactions: the birth of the hydrogen bond, Angew. Chem. Int. Ed. 44 (2005) 2356–2360.
[28] N. Faginas-Lago, F. Huarte Larrañaga, M. Albertí, On the suitability of the ILJ function to match different formulations of the electrostatic potential for water-water interactions, Eur. Phys. J. D 55 (1) (2009) 75.
[29] M. Albertí, N. Faginas-Lago, A. Laganà, F. Pirani, A portable intermolecular potential for molecular dynamics studies of NMA-NMA and NMA-H_2O aggregates, Phys. Chem. Chem. Phys. 13 (18) (2011) 8422–8432.
[30] F. Pirani, S. Brizi, L.F. Roncaratti, P. Casavecchia, D. Cappelletti, F. Vecchiocattivi, Beyond the Lennard-Jones model: a simple and accurate potential function probed by high resolution scattering data useful for molecular dynamics simulations, Phys. Chem. Chem. Phys. 10 (2008) 5489–5503.
[31] V. Aquilanti, A. Lombardi, R.G. Littlejohn, Hyperspherical harmonics for polyatomic systems: basis set for collective motions, Theor. Chem. Acc. 111 (2004) 400–406.
[32] A. Lombardi, N. Faginas-Lago, A. Laganà, F. Pirani, S. Falcinelli, A bond-bond portable approach to intermolecular interactions: simulations for N-methylacetamide and carbon dioxide dimers, in: B. Murgante, O. Gervasi, S. Misra, N. Nedjah, A. Rocha, D. Taniar, B. Apduhan (Eds.), Computational Science and Its Applications - ICCSA 2012, Part I, Lect. Notes Comput. Sci. 7333, Springer, Berlin Heidelberg, 2012, pp. 387–400.
[33] S. Falcinelli, M. Rosi, P. Candori, F. Vecchiocattivi, A. Bartocci, A. Lombardi, N. Faginas-Lago, F. Pirani, Modeling the intermolecular interactions and characterization of the dynamics of collisional autoionization processes, in: B. Murgante, S. Misra, M. Carlini, C. Torre, H.-Q. Nguyen, D. Taniar, B. Apduhan, O. Gervasi (Eds.), Computational Science and Its Applications - ICCSA 2013, Lect. Notes Comput. Sci. 7971, Springer, Berlin Heidelberg, 2013, pp. 69–83.
[34] A. Lombardi, A. Laganà, F. Pirani, F. Palazzetti, N. Faginas-Lago, Carbon oxides in gas flows and earth and planetary atmospheres: state-to-state simulations of energy transfer and dissociation reactions, in: B. Murgante, S. Misra, M. Carlini, C. Torre, H.-Q. Nguyen, D. Taniar, B. Apduhan, O. Gervasi (Eds.), Computational Science and Its Applications - ICCSA 2013, Lect. Notes Comput. Sci. 7972, Springer, Berlin Heidelberg, 2013, pp. 17–31.
[35] N. Faginas-Lago, M. Albertí, A. Laganà, A. Lombardi, L. Pacifici, A. Costantini, et al. The molecular stirrer catalytic effect in methane ice formation, in: B. Murgante, S. Misra, Computational Science and Its Applications-ICCSA 2014, Part I, Lect. Notes Comput. Sci. 8579, Springer International Publishing. 2014, pp. 585–600.
[36] N. Faginas-Lago, A. Lombardi, M. Albertí, G. Grossi, Accurate analytic intermolecular potential for the simulation of Na^+ and K^+ ion hydration in liquid water, J. Mol. Liq. 204 (2015) 192–197.
[37] N. Faginas-Lago, M. Albertí, A. Costantini, A. Laganà, A. Lombardi, L. Pacifici, An innovative synergistic grid approach to the computational study of protein aggregation mechanisms, J. Mol. Liq. 20 (7) (2014) 2226.
[38] L. Pacifici, M. Verdicchio, N. Faginas-Lago, A. Lombardi, A. Costantini, A high-level ab initio study of the $N_2 + N_2$ reaction channel, J. Comput. Chem. 34 (31) (2013) 2668–2676.
[39] M. Bartolomei, F. Pirani, A. Laganà, A. Lombardi, A full dimensional grid empowered simulation of the $CO_2 + CO_2$ processes, J. Comput. Chem. 33 (2012) 1806.
[40] A. Lombardi, N. Faginas-Lago, L. Pacifici, A. Costantini, Modeling of energy transfer from vibrationally excited CO_2 molecules: cross sections and probabilities for kinetic modeling of atmospheres, flows, and plasmas, J. Phys. Chem. A 117 (45) (2013) 11430–11440.
[41] A. Lombardi, N. Faginas-Lago, L. Pacifici, G. Gaia, Energy transfer upon collision of selectively excited CO_2 molecules: state-to-state cross sections and probabilities for modeling of atmospheres and gaseous flows, J. Chem. Phys. 143 (2015) 034307.
[42] N. Faginas-Lago, M. Albertí, A. Lombardi, A. Laganà, et al. Ion-water cluster molecular dynamics using a semiempirical intermolecular potential, in: B. Murgante, S. Misra, Computational Science and Its Applications-ICCSA 2015, Lect. Notes Comput. Sci. 9156, Springer International Publishing. 2014, pp. 355–370.
[43] M. Albertí, N. Faginas-Lago, F. Pirani, Benzene water interaction: from gaseous dimers to solvated aggregates, Chem. Phys. 399 (2012) 232–239.
[44] M. Albertí, N. Faginas-Lago, Ion size influence on the Ar solvation shells of $M^+C_6F_6$ clusters (M = Na, K, Rb, Cs), J. Phys. Chem. A 116 (2012) 3094–3102.
[45] A. Lombardi, F. Pirani, A. Laganà, M. Bartolomei, Energy transfer dynamics and kinetics of elementary processes (promoted) by gas-phase CO_2-N_2 collisions: selectivity control by the anisotropy of the interaction, J. Comput. Chem. 37 (16) (2016) 1463–1475.
[46] N. Faginas-Lago, M. Albertí, A. Lombardi, F. Pirani, A force field for acetone: the transition from small clusters to liquid phase investigated by molecular dynamics simulations, Theor. Chem. Accounts 135 (2016) 161.
[47] N. Faginas Lago, M. Albertí, A. Laganà, A. Lombardi, Water $(H_2O)_m$ or benzene $(C_6H_6)_n$ aggregates to solvate the K^+, Computational Science and Its Applications - ICCSA 2013, Part I, Lect. Notes Comput. Sci. vol. 7971, Springer-Verlag. 2013, pp. 1–15.
[48] M. Albertí, N. Faginas-Lago, Competitive solvation of K^+ by C_6H_6 and H_2O in the $K^+(C_6H_6)$n-(H_2O)m (n = 1–4; m = 1–6) aggregates, Eur. Phys. J. D 67 (4). (2013)
[49] M. Albertí, N.F. Lago, F. Pirani, Ar solvation shells in K + HFBz: from cluster rearrangement to solvation dynamics, J. Phys. Chem. A 115 (40) (2011) 10871–10879.
[50] S. Pallottelli, S. Tasso, N. Pannacci, A. Costantini, N. Faginas-Lago, Distributed and collaborative learning objects repositories on grid networks, Computational Science and Its Applications - ICCSA 2010, Part IV, Lect. Notes Comput. Sci. 6019, Springer-Verlag. 2010, pp. 29–40.
[51] R. Schweitzer-Stenner, G. Sieler, N. Mirkin, S. Krimm, Intermolecular coupling in liquid and crystalline states of trans-N-methylacetamide investigated by polarized Raman and FT-IR spectroscopies, J. Phys. Chem. A 103 (1998) 118–127.
[52] T. Whitfield, S. Martyna, G.J. Allison, S. Bates, H. Vass, J. Crain, Structure and hydrogen bonding in neat N-methylacetamide: classical molecular dynamics and Raman spectroscopy studies of a liquid of peptidic fragments, J. Phys. Chem. B 110 (2006) 3624–3637.
[53] D. Case, T. Cheatham, III, T. Darden, H. Gohlke, R. Luo, K. Merz, Jr, A. Onufriev, C. Simmerling, B. Wang, R. Woods, The Amber biomolecular simulation programs, J. Comput. Chem. 26 (2005) 1668–1688.
[54] A. Wallqvist, O. Teleman, Properties of flexible water models, Mol. Phys. 74 (1991) 515–533.
[55] M. Albertí, A. Aguilar, J.M. Lucas, F. Pirani, A generalized formulation of ion–electron interactions: role of the nonelectrostatic component and probe of the potential parameter transferability, J. Phys. Chem. A 114 (44) (2010) 11964–11970.
[56] M. Albertí, Rare gas-benzene-rare gas interactions: structural properties and dynamic behavior, J. Phys. Chem. A 114 (2010) 2266–2274.

[57] M. Albertí, F. Pirani, Features of Ar solvation shells in neutral and ionic clustering: the competitive role of two-body and many-body interactions, J. Phys. Chem. A 115 (2011) 6394–6404.
[58] M. Albertí, A. Aguilar, M. Bartolomei, D. Cappelletti, A. Laganà, J.M. Lucas, F. Pirani, A study to improve the van der Waals component of the interaction in water clusters, Phys. Scr. 78 (2008) 058108.
[59] M. Albertí, A. Aguilar, D. Cappelletti, A. Laganà, F. Pirani, On the development of an effective model potential to describe water interaction in neutral and ionic clusters, Int. J. Mass Spectrom. 280 (2009) 50–56.
[60] F. Pirani, M. Albertí, A. Castro, M. Moix, D. Cappelletti, Atom-bond pairwise additive representation for intermolecular potential energy surfaces, Chem. Phys. Lett. 394 (2004) 37.
[61] W. Smith, C. Yong, P. Rodger, DL_POLY: application to molecular simulation, Mol. Simul. 28 (5) (2002) 385–471.
[62] M.P. Allen, D.J. Tildesley, Computer Simulations of Liquids, Clarendon Press, Oxford, 1989.
[63] S. Trabelsi, F. Ammami, S. Nasr, M.-C. Bellissent-Funel, Neutron and X-ray scattering experiments on fully deuterated liquid N-methylacetamide $CD_3CONDCD_3$ at various temperatures and under pressure, J. Mol. Struct. 891 (1–3) (2008) 388–395.
[64] R. Ludwig, F. Weinhold, T.C. Farrar, Structure of liquid N-methylacetamide: temperature dependence of NMR chemical shifts and quadrupole coupling constants, J. Phys. Chem. A 101 (1997) 8861–8870.
[65] M. Hueselkopf, R. Ludwig, Correlations between structural, NMR and IR spectroscopic properties of N-methylacetamide, Magn. Reson. Chem. 39 (2001) 127–134.
[66] S. Trabelsi, M. Bahri, S. Nasr, X-ray scattering and density-functional theory calculations to study the presence of hydrogen-bonded clusters in liquid N-methylacetamide, J. Chem. Phys. 122 (2) (2005) 024502.
[67] G.J. Kearley, M.R. Johnson, M. Plazanet, E. Suard, J. Chem. Phys. 115 (2001) 2614–2620.
[68] R. Zhang, H. Li, Y. Lei, S. Han, Structures and interactions in N-methylacetamide-water mixtures studied by IR spectra and density functional theory, J. Mol. Struct. 693 (2004) 17–25.
[69] Y.A. Mantz, H. Gerard, R. Iftimie, G.J. Martyna, Ab initio and empirical model MD simulation studies of solvent effects on the properties of N-methylacetamide along a cis-trans isomerization pathway, J. Phys. Chem. B 110 (2006) 13523–13538.
[70] G. Jiali, F. Marek, Hybrid ab initio QM/MM simulation of N-methylacetamide in aqueous solution, J. Phys. Chem. A 101 (1997) 3182–3188.